ANALES DE LA REAL ACADEMIA NACIONAL DE FARMACIA
ISSN (Online) 1697-4298
Article
analesranf.com

Nannocannabinoids for brain tumor drug delivery

Title in Spanish: *Nanocannabinoides como terapia frente a glioma*

Juan Aparicio Blanco[1,*], Ignacio A. Romero[2], Jean P Benoit[3], Ana I. Torres Suárez[1]

[1]Departamento de Farmacia Galénica y Tecnología Alimentaria, Facultad de Farmacia, Universidad Complutense de Madrid, Spain. [2]Faculty of Science, Technology, Engineering & Mathematics, The Open University, Walton Hall, Milton Keynes MK7 6AA, United Kingdom. [3]MINT, UNIV Angers, INSERM 1066, CNRS 6021, Université Bretagne Loire, Angers, France.

ABSTRACT: Brain diseases are a major health challenge as brain drug delivery is truly hindered by the blood-brain barrier. Therefore, targeted drug nanocarriers arise as an alternative to achieve efficient transport across the brain endothelium following minimally-invasive intravenous injection. However, the global translational impact of nanomedicine remains modest. Certainly, the transition from empirical development towards a rational design tailored to the specific disease needs is likely to improve the chances of success.

Under this assumption and taking advantage of both the natural brain tropism and the antiproliferative activity of cannabidiol, to contribute to the rational design of targeted nanocapsules for glioma therapy, we have thoroughly screened the influence of distinct parameters on their *in vitro* and *in vivo* behaviour. Effectively, we have demonstrated that both the brain and glioma targeting ability and the drug release rate can be tailored by varying the particle size of the nanocapsules. This fine size-tailoring can be achieved by the phase inversion temperature method thanks to the herein-described linear univariate mathematical model as a function of the oily phase/surfactant mass ratio.

Moreover, we have introduced, on the one hand, a pioneering brain tumor targeting strategy with cannabidiol (with better targeting properties than other strategies that have already reached the clinical trials stage) and, on the other hand, nanocapsules as extended-release carriers of cannabidiol to overcome the formulation problems that have traditionally constrained its therapeutic potential.

Altogether, small lipid nanocapsules loaded and functionalized with cannabidiol arise as promising dually-targeted candidates for intravenous treatment of glioma.

RESUMEN: Las patologías cerebrales representan un desafío terapéutico por la restricción al paso de fármacos a través de la barrera hematoencefálica. Por ello, actualmente se persigue diseñar transportadores de fármacos capaces de atravesar de manera eficiente el endotelio cerebral tras su administración intravenosa. Sin embargo, el impacto traslacional de la nanomedicina es aún discreto. Sin duda, la transición de un desarrollo empírico hacia un diseño racional adecuado a las necesidades terapéuticas concretas en cada caso aumentará las posibilidades de éxito.

Bajo esta premisa y aprovechando tanto el tropismo cerebral como la actividad antiproliferativa del cannabidiol, y a fin de contribuir al diseño racional de nanocápsulas dirigidas para el tratamiento de gliomas, hemos evaluado la influencia de distintos parámetros en su comportamiento *in vitro* e *in vivo*. Efectivamente, hemos demostrado que tanto el paso a través de barrera hematoencefálica como la captación por células de glioma, así como la velocidad de liberación de fármacos pueden modularse variando su tamaño de partícula. El método térmico de inversión de fases posibilita la obtención de nanocápsulas bajo demanda en términos de tamaño gracias al modelo matemático lineal en una variable aquí descrito.

Además, hemos desarrollado una novedosa estrategia de vectorización con cannabidiol (que incluso supera a otras que ya se encuentran en ensayos clínicos). Asimismo, las nanocápsulas sirven como transportadores de liberación prolongada del cannabidiol, superando así sus problemas de formulación que venían limitando su potencial terapéutico.

En conjunto, las nanocápsulas lipídicas, cargadas y funcionalizadas con cannabidiol, constituyen prometedores candidatos para el tratamiento de gliomas.

*Corresponding Author: juan_ab89@hotmail.com
An Real Acad Farm Vol. 85, Nº 2 (2019), pp. 198-216
Received: May 7, 2019 Accepted: May 8, 2019
Language of Manuscript: English
Premio Juan Abelló del Concurso Científico 2018 de la Real Academia Nacional de Farmacia

1. INTRODUCTION

Brain diseases should be considered a major health challenge as brain drug delivery is truly hindered by the blood-brain barrier (BBB) (1). The BBB consists of the endothelium of brain capillaries. The key features of the brain endothelium that severely restrict brain drug delivery are both the lack of fenestrations and the presence of tight intercellular junctions. Hence, there is a dire need for developing effective brain drug delivery strategies that overcome the biodistribution limitations that account for treatment failure (2).

Some of the described delivery strategies to circumvent the BBB such as the intracerebral administration and the artificial disruption of the tight junctions involve high risk of neurological damage and even of widespread tumor dissemination in the case of brain tumors. Therefore, the use of targeted drug nanocarriers arises as a promising alternative to achieve efficient transport across the brain endothelium following minimally-invasive intravenous injection (3-5).

Unfortunately, the global translational impact of nanomedicine remains modest. In this context, we have analyzed the possibilities and technological challenges ahead to improve the chances of success in the development of nanomedicines for brain pathologies. Certainly, whereas the empirical development of delivery systems and their subsequent application to a specific disease has led to high attrition rates in clinical trials, the transition towards a disease-driven approach, whereby the nanomedicine features are rationally defined beforehand based on the pathophysiology of a specific disease is more likely to succeed.

One of the major features that influence the *in vivo* behaviour of nanocarriers is particle size as their effect mainly relies on the unique interactions of materials at the nanoscale with biological structures. For instance, a size-driven extravasation at tumor and/or inflammatory sites based on their pathophysiological features (namely, the enhanced permeation and retention (EPR) effect) has been sought. However, the EPR effect in brain diseases is relatively weak due to the presence of the BBB, with a cut-off size of only 10-100 nm (6). In these cases, a much finer control over particle size will certainly improve the potential therapeutic benefits. Hence, rational disease-driven design of nanocarriers can only be achieved by determining the parameters that accurately control their size distribution.

Under this assumption, we have thoroughly studied which parameters control the size distribution of lipid nanocapsules (LNCs) prepared by the phase inversion temperature (PIT) method. The PIT method is a low-energy nanoemulsification method wherein the physicochemical properties of surfactants are exploited to lower the required energy input for nanoemulsification according to the Young-Laplace equation for a spherical drop. To this end, the PIT method profits from the negligible interfacial tension achieved when the surfactant curvature is inverted by changes in temperature. At the "phase inversion temperature", the affinity for both phases is balanced and the minimum in interfacial tension is achieved (7). As the final formulation is obtained following a thermal quench below the surfactant melting point, nanoemulsions eventually adopt the form of nanocapsules with a liquid oily core stabilized by a rigid surfactant shell.

With around a quarter of a million new cases of brain tumors every year, these brain diseases could take great advantage of LNCs. Brain tumors are stratified according to a 'malignancy scale' (8). Malignant primary brain tumors typically originate from glial cells (being thus referred to as gliomas). The current standard approach in high grade gliomas combines maximal surgical resection (if eligible) with radiotherapy and chemotherapy; as well as symptomatic treatment. Unfortunately, the efficacy of this treatment remains questionable, since recurrence happens within months after diagnosis, with a median survival of 14.6 months (9).

In the search for novel antitumor agents, the therapeutic potential of several cannabinoids has become a research hotspot as they have been reported to not only palliate cancer-related symptoms (such as nausea, pain or anorexia) but also promote apoptotic cancer cell death, impair tumor angiogenesis and reduce cell migration (10, 11). Cannabinoids are pharmacologically-active terpenophenols that can be ascribed to three distinct categories: phytocannabinoids (produced by the glandular trichomes of the herbaceous plant *Cannabis sativa* (12)), endocannabinoids (produced naturally by animals and humans) and synthetic cannabidomimetics (13). However, the therapeutic potential of cannabinoids has been truly constrained heretofore due to their strong psychoactive effects and their high lipophilicity.

Precisely due to the lack of these psychoactive effects, cannabidiol (CBD) arises as the phytocannabinoid with the greatest potential to widen the therapeutic armamentarium for the treatment of gliomas thanks to its synergism with the currently available chemo and radiotherapy (14). As a proof of it, CBD has reached the clinical trials stage as adjuvant therapy for patients with glioblastoma (ClinicalTrials.gov identifiers: NCT01812616, NCT01812603, NCT03246113 and NCT03529448).

Moreover, cannabinoids can take great advantage of nanomedicine-based formulation strategies to overcome the dosing problems traditionally associated with their high lipophilicity. Accordingly, several studies on nanocarriers encapsulating different kinds of cannabinoids have been published for distinct therapeutic purposes (Table 1). Notwithstanding that for cannabinoids to achieve high translational impact they should be devoid of psychoactive effects; the focus so far has been mainly put on 9-delta-tetrahydrocannabinol (Δ^9-THC) and its analogues. Hence, we have evaluated herein LNCs as biocompatible carriers for CBD.

Table 1: Published articles on the encapsulation of different kinds of cannabinoids within nanocarriers. $^{9}\Delta$-THC: 9-delta-tetrahydrocannabinol, AEA: anandamide.

Cannabinoid	Type of cannabinoid	Carrier	Therapeutic potential	Ref
$^{9}\Delta$-THC	Phytocannabinoid	Mesoporous silica nanoparticles	*In vivo* neuropathic pain relief	(15)
$^{9}\Delta$-THC	Phytocannabinoid	PLGA nanoparticles	*In vitro* and *in vivo* chemotherapy for lung cancer	(16)
$^{9}\Delta$-THC	Phytocannabinoid	PLGA nanoparticles	*In vitro* chemotherapy for colon adenocarcinoma	(17)
$^{9}\Delta$-THC and CBD	Phytocannabinoid	Nanolipospheres	-	(18)
AEA	Endocannabinoid	Poly-ε-caprolactone nanoparticles	-	(19)
Rimonabant	Synthetic cannabidomimetic	Nanostructured lipid carriers	-	(20)
Rimonabant, URB597 and AM251	Synthetic cannabidomimetic	Nanostructured lipid carriers	-	(21)
WIN55,212-2	Synthetic cannabidomimetic	Styrene maleic acid micelles	*In vivo* neuropathic pain relief	(22)
Dexanabinol	Synthetic cannabidomimetic	Solid lipid nanoparticles	*In vivo* antidepressant effect	(23)
CB13	Synthetic cannabidomimetic	PLGA nanoparticles	*In vivo* neuropathic pain relief	(24)
CB13	Synthetic cannabidomimetic	PLGA nanoparticles	-	(25, 26)
CB13	Synthetic cannabidomimetic	Lipid nanoparticles	-	(25, 27)

To be efficacious following intravenous administration, these carriers must be able to traverse the BBB to ultimately reach the tumor cells. Unfortunately, although the paracellular permeability of the brain endothelium is altered in most brain diseases, this disruption only occurs substantially in advanced stages of disease and in the most affected regions (28, 29). Therefore, brain targeting should not solely rely on passive targeting. Alternatively, brain active targeting is being explored to boost the transcellular delivery efficiency of nanocarriers across the BBB (30).

Brain active targeting is based on the modification of nanocarriers with moieties that trigger receptor-mediated transcytosis into the central nervous system (CNS) through specific binding with transporters overexpressed on the brain endothelium. Although numerous receptors have been used to design brain active targeting strategies across the BBB, the translational impact of brain active targeting remains modest, as only three actively-targeted liposomes have reached the clinical trials stage for distinct brain conditions (ClinicalTrials.gov identifiers: NCT01386580, NCT02048358 and NCT02340156) due to the flaws of the currently available targeting moieties (namely, the development of competitive phenomena with endogenous ligands and/or of immunogenicity) (31, 32).

Therefore, research on novel exogenous non-immunogenic moieties is likely to thrive shortly. In this respect, CBD has been reported to bind to various receptors located on the brain endothelium environment: namely, cannabinoid receptors CB_1 (33) and CB_2 (34), serotoninergic receptor 5-HT_{1A} (35), transient potential vanilloid receptors $TRPV_{1–2}$ (36), glycine receptor (37), adenosine receptor A_{2A} (38), G-protein-coupled receptor 55 GPR55 (39) and dopamine receptor D_2 (40)).

Apart from those receptors normally overexpressed on the brain endothelium, those overexpressed on tumor cells can also be used for active targeting of brain tumors to promote the selective distribution to glioma cells. In this respect, the expression of some of the receptors to which the cannabinoids bind has been reported to be increased in glioma (namely, cannabinoid receptors 1 and 2 (CB_1 and CB_2) (41), transient potential vanilloid receptor type 2 (TRPV2) (36) and G-protein-coupled receptor 55 (GPR55) (42).

Hence, we have designed two distinct strategies to incorporate CBD in the aforesaid size-tailored LNCs for glioma therapy depending on the ultimate therapeutic purpose. On the one hand, we have introduced herein a pioneering functionalization strategy for brain tumor targeting of LNCs with CBD under the assumption that, if existing, this double BBB- and glioma-targeting effect will ultimately enable a dual-targeting strategy for intravenous treatment of glioma to be achieved. The BBB-targeting efficiency of this active targeting strategy has been explored *in vitro* and *in vivo*, whereas the glioma-targeting efficiency has been assessed *in vitro* with the human glioblastoma cell line U373MG. As the mechanisms that drive the distinct active targeting strategies may follow a

size-dependent pattern, the role played by the particle size of LNCs in the extent of targeting has concomitantly been evaluated. On the other hand, we have encapsulated CBD into the oily core of LNCs and assessed *in vitro* their efficacy as extended-release carriers of CBD against the U373MG cell line. The role played by the size of LNCs in drug release and cytotoxicity has also been evaluated..

2. MATERIALS AND METHODS

2.1. Materials

Labrafac® lipophile WL 1349 (caprylic-capric acid triglycerides) and Labrafil® M 1944 CS (6-macrogol oleic glycerides) *were* kindly supplied by Gattefossé. Kolliphor® HS15 ($C_{18}E_{15}$ polyethylene glycol (15) 12-hydroxystearate) and Kolliphor® ELP ($C_{18\Delta9}E_{35}$ polyethylene glycol (35) ricinoleate) were gifts from BASF. Lipoid® S75 (soybean lecithin with 70% of phosphatidylcholine) was supplied by Lipoid-Gmbh. NaCl was purchased from Panreac. De-ionized water was obtained from a MilliQ® Purification System. The fluorescent dyes 3,3'-dioctadecyloxacarbocyanine perchlorate (DiO) and 1,1′-dioctadecyl-3,3,3′,3′-tetramethylindodicarbocyanine 4-chlorobenzenesulfonate salt (DiD) were purchased from Invitrogen Molecular Probes. Cannabidiol (CBD) was provided by THC-Pharma. Endothelial Cell Basal Medium-2 (EBM-2) and its culture supplements were purchased from Lonza. Dulbecco's Modified Eagle Medium (DMEM) and penicillin-streptomycin (10,000 U/mL) were provided by Gibco. Tetramethyl-rhodamine-isothiocyanate–dextran (TRITC-dextran, MW 150 kDa), type I collagen from calf skin, fibronectin from bovine plasma, Hank's Balanced Salt Solution (HBSS), 3-(4,5-dimethyl-2-thiazolyl)-2,5-diphenyl-2H-tetrazolium bromide (MTT), dimethyl-sulfoxide (DMSO) and sterile Nunc Lab-Tek® chamber slides (8 wells, Permanox® slide, 0.8 cm^2/well) were purchased from Sigma-Aldrich. Vectashield® mounting medium with DAPI (H-1200) was provided by Vector Laboratories. Sterile Millicell® Hanging Cell Culture Inserts (12-well culture plates; membrane: polyethylene terephthalate membrane; pore size: 1.0 μm; membrane surface area: 1.1 cm^2) and Amicon® Ultra 15 mL Centrifugal Filters (MWCO: 10 kDa) were supplied by Merck Millipore. Methanol, acetonitrile and tetrahydrofuran HPLC grade were purchased from Fisher Scientific.

2.2. Cell lines

The human brain endothelial hCMEC/D3 cells were seeded in collagen-coated flasks and cultured in EBM-2 medium supplemented with 2.5% foetal bovine serum (FBS), 0.025% (v/v) rhEGF, 0.025% (v/v) VEGF 0.025% IGF, 0.1% (v/v) rhFGF, 0.1% (v/v) gentamycin, 0.1% (v/v) ascorbic acid and 0.04% (v/v) hydrocortisone at 37ºC and 5% CO_2. For all experiments, cells between passage 25 and 30 were used.

The human glioblastoma U373MG cells were cultured in DMEM medium supplemented with 10% FBS, 100 U/mL penicillin and 100 μg/mL streptomycin at 37ºC and 5% CO_2. For all experiments, cells between passage 15 and 25 were used.

2.3. Animals

Male ICR mice (4-5 weeks old) were purchased from Envigo. The mice were housed in ventilated cages with free water and food in a 12h dark/light cycle. All *in vivo* experiments were approved by the Ethics Committee of the Community of Madrid (Ref. PROEX 111/14) and conducted according to Spanish and European guidelines (Directive 86/609/EEC).

2.4. Preparation and characterization of LNCs

LNCs were prepared by the PIT method (43). Briefly, all excipients (namely, aqueous and oily phases along with nonionic polyethoxylated surfactants) were mixed under magnetic stirring and progressively heated over the phase inversion temperature of the system. Subsequently, the mixture was gradually cooled down until the phase inversion temperature was reached. Then, a sudden quench with cold water (5 mL) was performed to obtain the final suspension of LNCs. Different formulations of LNCs were prepared by varying the relative proportions of their excipients and the surfactant/oil affinity, i.e. changing the nature of the surfactant (between Kolliphor® HS15 and Kolliphor® ELP) and of the oil (between Labrafac® lipophile WL1349 and Labrafil® M 1944 CS).

2.4.1. Size distribution and zeta potential

The average volume diameter and polydispersity index (PdI) were measured by dynamic light scattering (DLS) with a Microtrac® Zetatrac™ Analyzer (Microtrac Inc.). The zeta potential was measured using a Zetasizer Nano ZS (Malvern Instruments).

2.4.2. Incorporation efficiency and drug content

The CBD content in the CBD-decorated and CBD-loaded LNCs was determined by high performance liquid chromatography (HPLC). A mixture of methanol: acetonitrile: water (52:30:18 v/v) at a flow rate of 1.8 mL/min was used as mobile phase. The analytical column was a reversed-phase Mediterranea Sea® C18 (5μm 15 x 0,46 cm) (Teknokroma®). The amount of CBD associated with LNCs in each case was determined as the difference between the total amount of CBD in suspension derived from the lysis of LNCs with tetrahydrofuran (1:5 (v/v)) and the unassociated CBD filtered with 10 kDa Amicon® Centrifugal Filters (6000 rpm, 60 min).

2.5. In vitro evaluation of the BBB and glioma targeting ability of the CBD functionalization strategy

2.5.1. CBD decoration of LNCs

The fluorescent dye DiO was encapsulated in LNCs for *in vitro* experiments. To this end, the fluorescent dye was dissolved in the oily core of the LNCs at a weight ratio of 15 mg of dye/g of Labrafac® WL1349. Pre-formed fluorescently-labeled LNCs were incubated with a CBD solution (15 mg/mL) in a 3:1 (v/v) ratio. The mixture was gently stirred overnight until complete solvent

evaporation.

2.5.2. Uptake experiments

Flow cytometry was used to quantitatively evaluate the BBB and glioma targeting ability *in vitro*. hCMEC/D3 and U373MG cells were separately seeded into 6-well plates. After cells had been confluent for 48 hours, the culture medium was replaced by fluorescently-labeled LNCs at an equivalent dye concentration of 1.65 µg DiO/mL of medium. After 24 hours incubation, cells were rinsed, trypsinized and finally resuspended in 0.3 mL of HBSS. The fluorescence intensity of cells treated with fluorescent-LNCs was analyzed with a flow cytometer (FACScalibur, BD Biosciences). Cells treated with blank LNCs served as control.

Confocal microscopy was used to qualitatively illustrate the BBB and glioma targeting ability *in vitro*. hCMEC/D3 and U373MG cells were separately seeded into chamber slides. After cells had been confluent for 48 hours, the culture medium was replaced by fluorescently-labeled LNCs at an equivalent dye concentration of 1.65 µg DiO/mL of medium. After 24 hours incubation, cells were rinsed and mounted with Vectashield® with DAPI mounting medium. The cells were then observed with a Leica SP5 microscope (405 nm for DAPI, 488 nm for DiO). Cells treated with blank LNCs served as control. 3D imaging reconstruction was made with IMARIS software.

2.5.3. BBB permeability experiments

hCMEC/D3 cells were seeded into collagen- and fibronectin-coated hanging cell culture inserts at confluence and incubated for 72 hours in complete EBM-2. The monolayer integrity was assessed by determining the permeability coefficient across the hCMEC/D3 monolayer of TRITC-dextran both in the presence and the absence of LNCs. Briefly, a TRITC-dextran solution (2 mg/mL) was added in the apical chamber and at 2, 4, 6, 8, 12 and 24 hours, 200 µL from the basolateral compartment were sampled and replaced with fresh medium. At 24 hours, the apical compartment was likewise sampled (100 µL). Similarly, in a separate experiment, fluorescently-labeled LNCs at an equivalent dye concentration of 1.65 µg DiO/mL were added in the apical chamber to determine the permeability coefficient of the different formulations across the hCMEC/D3 monolayer. The concentration of TRITC-dextran and DiO were determined using a microplate reader (FLUOstar Omega, BMG Labtech; λ_{exc} dextran: 544 nm, λ_{em} dextran: 590 nm, λ_{exc} DiO: 485 nm, λ_{em} DiO: 520 nm). These concentrations were used to calculate the permeability coefficients using the equations from (44).

2.6. In vivo evaluation of the BBB targeting ability of CBD-decorated LNCs

For biodistribution studies in healthy mice, DiO was replaced by the fluorescent dye DiD. Mice (n=4-5 per group) were injected via the tail vein with 150 µL of DiD-fluorescently-labeled LNCs. Ninety minutes after administration, mice were sacrificed, and the brain, liver, spleen, kidneys, lungs, heart and blood were collected and homogenized in ethanol for dye extraction. The concentration of DiD was measured using a microplate reader (Varioskan Flash, Thermo Scientific, excitation wavelength: 644 nm, emission wavelength: 665 nm). Results were expressed as percentage of the injected dose per gram of organ.

2.7. In vitro efficacy of CBD-loaded LNCs against U373MG cells

2.7.1. CBD loading into the LNCs core

CBD was encapsulated in the oily core of LNCs for *in vitro* efficacy experiments by dissolving it at a concentration of 15 % CBD/ Labrafac® WL1349 (w/w). Then, the remaining excipients were added and progressively heated and cooled down around the phase inversion temperature as indicated above.

2.7.2. Cytotoxicity experiments

U373MG cells were seeded into 96-well plates. After 48 hours of incubation, cells were treated with LNCs (200 µL) for 48 and 96 hours. Then, the *in vitro* cytotoxicity of CBD-loaded LNCs was determined using an MTT assay. For each formulation of CBD-loaded LNCs, U373MG cells treated with their blank counterparts served as control. Cell viability was expressed as a percentage relative to that of control. The half-maximal inhibitory concentration (IC_{50}) was calculated in each case.

2.8. Statistical analysis

The data are expressed as mean ± SD of at least three different experiments. Unpaired Student's t test was used for two-group comparisons. One-way ANOVA followed by post-hoc Tukey test were used for multiple-group analysis. Statistical significance was fixed as *: $p<0.05$, **: $p<0.01$, ***: $p<0.001$. All the data were analyzed using the GraphPad Prism 7 software.

3. RESULTS AND DISCUSSION

3.1. Determination of the parameters that control the size distribution of LNCs prepared by the PIT method

The parameters that control the properties of nanocarriers can be classified into formulation or preparation variables. For low-energy methods (as it is the case of the PIT method), the formulation variables, and particularly the relative proportion of excipients, are the key parameters, as these methods do not rely either on physical energy input or on shear forces. Since Morales et al (45) showed that water only acts as a dilution medium for the dispersed phase, we hypothesized that surfactant and oil should be considered the formulation-driving parameters. In this respect, particle size is expected to be reduced with increasing amounts of surfactant due to the decrease in interfacial tension and to grow with increasing amounts of oil, as it constitutes the liquid core of the nanocapsules. As a result, the oily phase/surfactant mass ratio seems to be a suitable variable for prediction of the particle size of LNCs prepared by the PIT method.

Effectively, as shown in Figure 1 and Table 2, we have

evidenced herein that the oily phase/surfactant mass ratio is the major parameter that drives nanocapsule formation for different oil-surfactant combinations (namely, Labrafac® WL1349-Kolliphor® HS15, Labrafac® WL1349-Kolliphor® ELP, Labrafil® M 1944 CS-Kolliphor® HS15). These combinations exhibit distinct oil/surfactant affinities as summarized in Table 3 in terms of HLB. The plot of the average volume diameters versus the oil/surfactant ratio was linear within the ratio range between 0.08 and 3 and this linear trend is consistent through the distinct surfactant-oil affinities. According to the high coefficients of determination observed (R^2>0.99), these univariate linear mathematical models are well-suited to predict the particle size of the nanocapsules prepared by the PIT method. As hypothesized, particle size increased along with the oil/surfactant ratio: higher ratios represent a decrease in surfactant relative concentration, and ultimately lead to bigger capsules. The estimation of particle size with a univariate mathematical model is of the greatest importance as it will intuitively teach formulators how to tailor particle size of LNCs prepared by the PIT method to the therapeutic needs imposed by a specific disease. Highly monodisperse LNCs were obtained in all cases: the polydispersity indexes (PdI) were maintained under 0.06, regardless the particle size, well below the most broadly used upper limit for monodisperse criteria of 0.1.

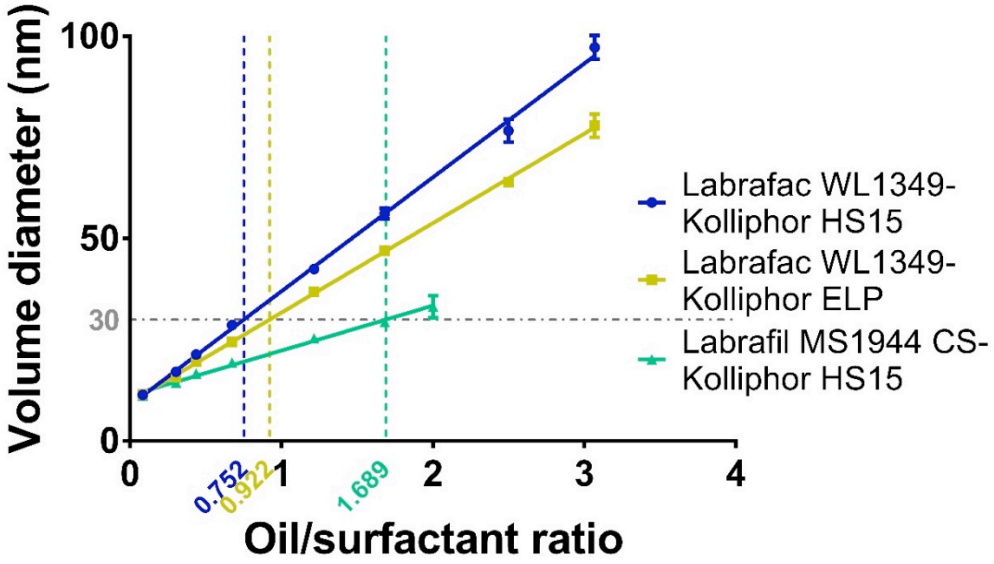

Figure 1: Univariate linear regression between the average volume diameter and the oil/surfactant mass ratio of LNCs prepared by the PIT method.

Table 2: Parameters of the univariate linear regression between the average volume diameter and the oil/surfactant mass ratio for the different combinations tested.

Oil/surfactant tandem	Y-intercept	Slope	R^2
Labrafac® lipophile WL1349- Kolliphor® HS15	8.83	28.16	0.9983
Labrafac® lipophile WL1349- Kolliphor® ELP	9.59	22.13	0.9996
Labrafil® M 1944 CS- Kolliphor® HS15	11.23	11.11	0.9939

Table 3: HLB values of the different oily phases and polyethoxylated surfactants as declared by suppliers.

Excipient	HLB value
Labrafac® lipophile WL1349	1
Labrafil® M 1944 CS	9
Kolliphor® ELP	13
Kolliphor® HS15	15

Importantly, a comparison among the linear plots for the different oil-surfactant tandems can be drawn. On the one hand, there are not statistically significant differences in the Y-intercept (Table 2), which means that there exists a lower limit of particle size to be obtained with the PIT method and this limit equals 10 nm. On the other hand, we

observe significant differences in the slopes (***: $p<0.001$). As shown in Table 2, the steepest slope was achieved for the Labrafac®-Kolliphor® HS15 tandem (b = 28.16), whereas the lowest value corresponded to the Labrafil®-Kolliphor® HS15 (b = 11.11). This difference in the slopes can be explained by the difference between the HLB values of the poly-ethoxylated surfactants and the triglycerides used as oily phase. The slopes follow this pattern: the closer the HLB affinity between the surfactant and the oily phase, the lower the slope of the linear plot.

As a result, the size of nanocapsules can be precisely tailored to each therapeutic purpose within the range of 10-100 nm. Importantly, since the univariate linear model has been established for surfactants and oily phases with different affinities, this tailoring can also be made in terms of adjusting the excipients to therapeutic needs. For example, solubility issues dictated by a given drug can presumably be addressed by changing the oily phase to one that fully solubilizes it. Alternatively, toxicological concerns related to a given surfactant can be overcome as nanocapsules of the same size can be obtained at a lower surfactant concentration by switching to an emulsifier with a lower HLB or by switching to an oily phase with a higher HLB. This can ultimately help increase the maximum tolerated dose. These latter cases are illustrated in Figure 1. For a given volume diameter, fixed in 30 nm, a formulation with a 0.752 ratio for the Labrafac® WL1349-Kolliphor® HS15 tandem can be used. However, according to our results, there are other alternatives. On the one hand, the Kolliphor® HS15 with a HLB of 15 can be switched to another poly ethoxylated surfactant with a lower HLB (namely, Kolliphor® ELP with a HLB of 13) and this change will imply a reduction in the surfactant amount, as it will require a higher oil/surfactant ratio (0.922). On the other hand, the oily phase can likewise be modified to ultimately reduce the amount of surfactant. The replacement of Labrafac® WL1349 with a HLB of 1 by Labrafil® M 1944 CS with a HLB of 9 will enable 30-nm sized nanocapsules to be obtained at an oil/surfactant ratio of 1.689, which halves the required amount of surfactant.

This finding refutes the broadly-agreed requirement for a surfactant with an optimum HLB number for a given oily phase. The reason may lie in the fact that the HLB number concept, defined at 25ºC, only considers the surfactant molecule itself and overlooks the interactions with the aqueous and oily phases under the influence of external parameters.

Furthermore, the linear univariate mathematical model serves to predict the particle size of nanocapsules prepared by other authors through not only the PIT method, but also through other phase inversion methods (Table 4). This unequivocally validates that the oil/surfactant mass ratio is the leading parameter that controls size distribution of final suspensions.

Table 4: Parameters of the univariate linear regression between the average volume diameter and the oil/surfactant mass ratio for the different combinations tested.

Preparation method	R^2	Ref.
Phase inversion temperature	0.9928	(46)
Phase inversion temperature	0.9908	(47)
Phase inversion temperature	1	(48)
Phase inversion composition	0.99	(49)
Phase inversion composition	0.9992	(50)
Phase inversion composition	0.993	(51)
Phase inversion composition	0.9789	(52)

Altogether, these results serve to envisage LNCs prepared by the PIT method as promising carriers for the treatment of brain diseases following a disease-driven design.

3.2. Determination of BBB and glioma targeting ability of fluorescently-labeled LNCs

Monodisperse LNCs with the Labrafac®-Kolliphor® HS15 tandem were prepared in two different sizes and loaded with fluorescent dyes for particle tracking purposes. Whereas the fluorescent dye DiO was encapsulated for *in vitro* experiments, we used the fluorescent dye DiD in *in vivo* experiments because it is excited and emits within the near-infrared window (namely, the wavelength range with the lowest absorption in tissue).

Both kinds of fluorescently-labeled LNCs were functionalized with CBD to assess the potential of this cannabinoid to enhance the brain tumor targeting properties. High CBD adsorption efficiencies were achieved with this functionalization strategy (Table S1), which doubled those reported by Balzeau et al with a targeting peptide following a similar procedure (53). These results could be explained by the lower aqueous solubility of CBD than that of peptides, which eventually favors its

adsorption at the amphiphilic interface.

Overall, the size distribution features of both types of fluorescently-labeled LNCs were analogous. As shown in Figure 2, the encapsulation of the fluorescent dyes did not alter the size of blank LNCs (20 nm and 40 nm, respectively). Conversely, the adsorption of CBD on fluorescently-labeled LNCs increased their particle size from 20 to 40 nm and from 40 to 55-60 nm. This increase followed an inverse size-related pattern: a 100%-increase for the smaller LNCs versus a 48%-increase for the bigger ones. The higher specific surface area of the smaller LNCs can account for this trend observed upon CBD functionalization. Moreover, the zeta potential profiles of CBD-adsorbed LNCs were noticeably sharpened in comparison with those of blank LNCs (Figure S1). These profiles support the superficial location of the adsorbed CBD.

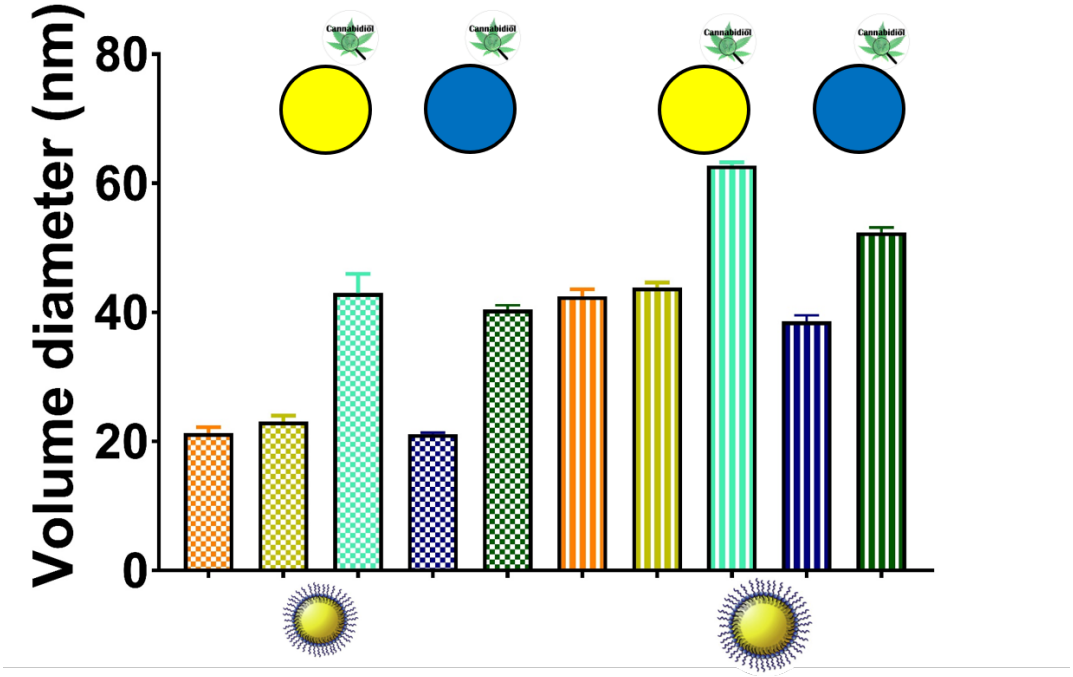

Figure 2: Average volume diameter of the different LNCs used to assess the BBB and glioma targeting ability: blank LNCs (orange), non-functionalized fluorescently-labeled LNCs (DiO: gold; DiD: navy blue) and CBD-adsorbed fluorescently-labeled LNCs (DiO: turquoise, DiD: green). For each formulation, there exist a smaller-sized (squared fill pattern) and a bigger-sized (striped fill pattern) counterpart.

The experimental design to assess the BBB and glioma targeting ability of LNCs was as follows. On the one hand, as the cell internalization mechanisms may follow a size-dependent pattern, the role played by particle size in the targeting properties has been assessed separately in undecorated and in CBD-adsorbed fluorescently-labeled LNCs. On the other hand, as the increase of particle size due to CBD adsorption within the 20-60 nm interval represents a higher percentage increase than in the most widely explored 100-nm range, should particle size play a statistically significant role in the targeting properties, the influence of CBD-decoration will be then evaluated for equally-sized LNCs to maintain the size variable constant.

The BBB-targeting ability has been evaluated through uptake and permeability experiments conducted with the human brain endothelial cell line hCMEC/D3. The results obtained with the *in vitro* cell-based BBB model have also been validated with *in vivo* biodistribution data in healthy mice.

The quantitative analysis of the *in vitro* BBB-targeting ability is shown in Figure 3. Results consistently demonstrated a significantly higher BBB-targeting effect for smaller LNCs (1.8-fold for undecorated LNCs, $p < 0.01$ and 2.0-fold for CBD-adsorbed LNCs, $p<0.01$). Given the influence of particle size on the BBB targeting ability, the role played by CBD-adsorption was then assessed from a comparison of equally-sized LNCs. The adsorption of CBD on LNCs enhanced by 1.4-fold ($p < 0.05$) the BBB targeting ability of their undecorated equally-sized counterparts. The 3D reconstructions from the Z-stacks of the images taken by confocal microscopy evidenced qualitatively a perinuclear location of the LNCs within the hCMEC/D3 cells (Figure 4).

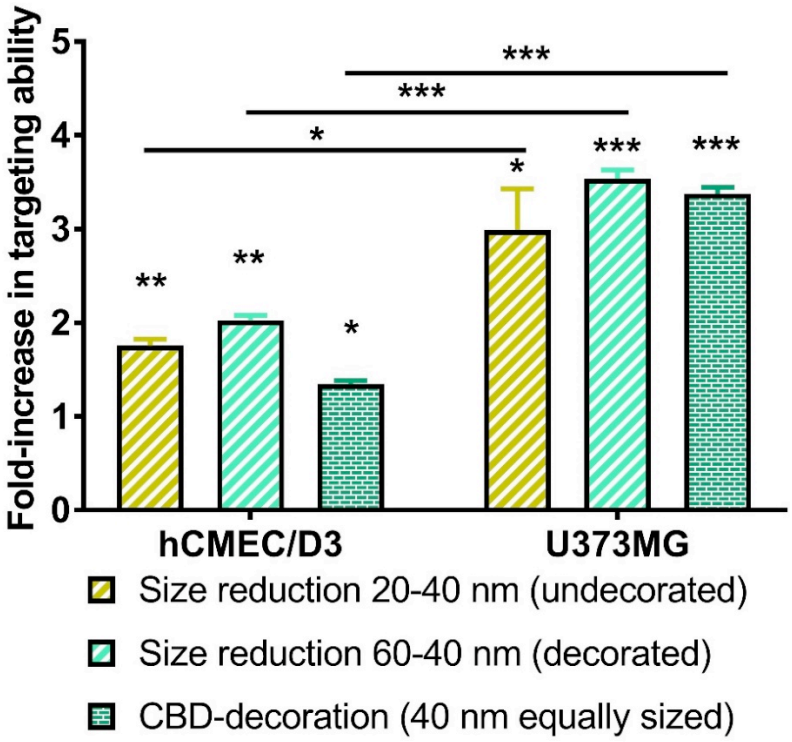

Figure 3: Quantitative analysis by flow cytometry of influence of particle size reduction and functionalization with CBD on the *in vitro* BBB (left) and glioma (right) targeting ability of LNCs. *: p<0.05, **: p<0.01, ***: p<0.001.

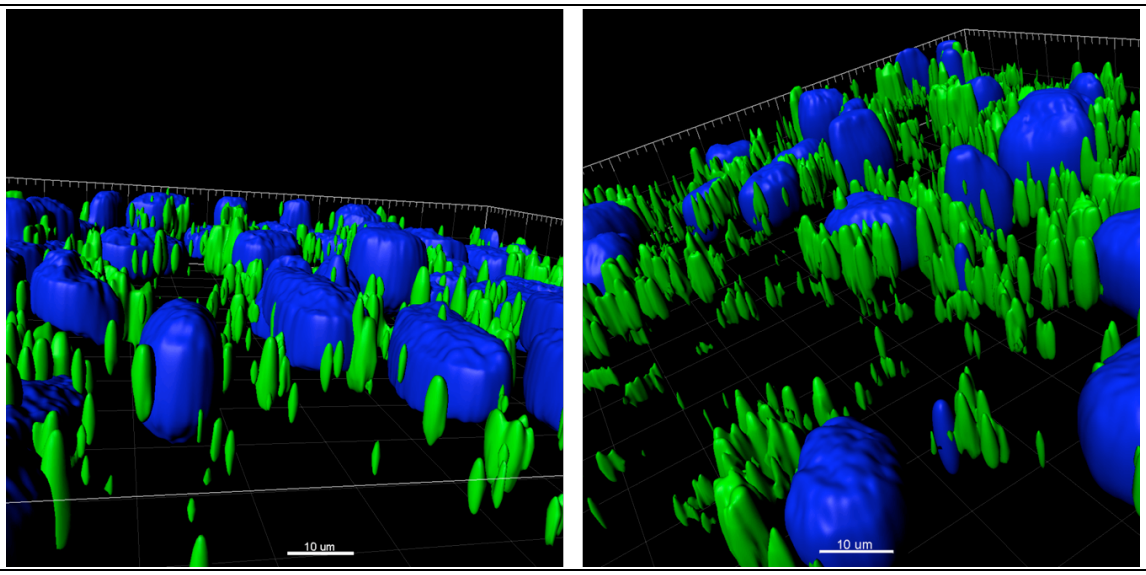

Figure 4: 3D reconstructions with the IMARIS software of the Z-stacks of confocal images with hCMEC/D3 cells: undecorated (left) and CBD-adsorbed (right) fluorescently-labeled LNCs. Scale bar = 10 µm.

Importantly, we verified that the nanocapsules themselves did not alter the barrier properties of the hCMEC/D3 monolayer before conducting the BBB permeability experiments with LNCs. Effectively, there were no statistically significant differences between the permeability coefficients of TRITC-dextran across the hCMEC/D3 monolayer in the presence and the absence of LNCs ($1.67 \pm 0.44 \times 10^{-7}$ cm/s versus $1.77 \pm 0.33 \times 10^{-7}$ cm/s, $p>0.05$). These results demonstrated the integrity of the BBB model throughout the 24 hours period evaluated and consequently the suitability of this model for evaluating the BBB transport ability of the LNCs.

The quantitative analysis of the *in vitro* BBB-permeability coefficients is shown in Figure 5. We have used herein the permeability coefficient as a robust parameter that readily enables the comparison of transport

efficiency (which is not the case for the transport ratio expressed as percentage of passage across the endothelial monolayer). Results from the permeability experiments were consistent with those obtained with uptake studies. The BBB permeability coefficients were significantly higher for smaller LNCs (2.8-fold for undecorated LNCs, $p < 0.01$ and 2.5-fold for CBD-adsorbed LNCs, $p < 0.001$). As particle size determined the permeability coefficient, the influence of CBD adsorption was then assessed from a comparison of equally-sized LNCs. The adsorption of CBD on LNCs enhanced by 5.2-fold ($p < 0.001$) the permeability coefficient of their undecorated equally-sized counterparts.

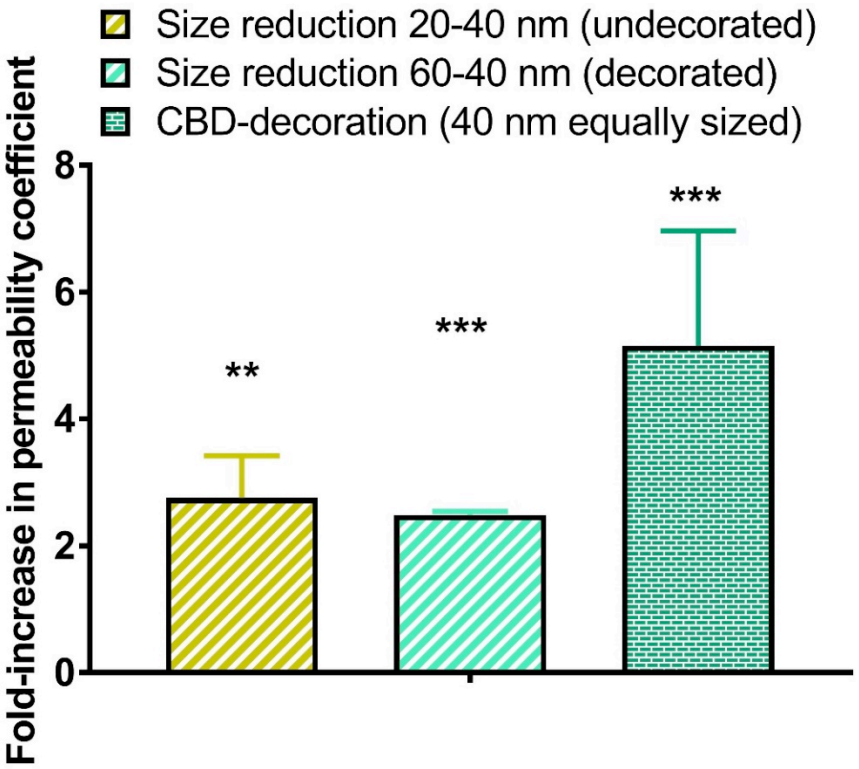

Figure 5: Quantitative analysis of influence of particle size reduction and functionalization with CBD on the permeability coefficient of LNCs of LNCs across the hCMEC/D3 monolayer. *: p<0.05, **: p<0.01, ***: p<0.001.

These results have been validated with biodistribution studies. Although pathophysiological models have often been used to evaluate the brain targeting efficiency, given that BBB disruption only occurs in the most damaged brain areas, we aimed at evidencing targeting properties at earlier stages of the brain diseases with biodistribution studies in healthy mice.

As the size distribution features of DiD-labeled LNCs were analogous to their DiO-labeled counterparts (Figure 2), the same comparisons as those drawn *in vitro* have been made *in vivo*. We have determined the percentage of the injected dose per gram of organ in brain (Figure 6), blood, lungs, kidneys, heart, spleen and liver (Figure S2).

The *in vivo* results confirmed the results obtained with the *in vitro* BBB model: a decrease in particle size yielded a higher transcytosis rate to brain (1.6-fold for undecorated LNCs, $p < 0.05$ and 2.2-fold for CBD-adsorbed LNCs, $p < 0.01$). Given the influence of particle size on the brain distribution, the influence of CBD adsorption was then assessed from a comparison of equally-sized LNCs. The functionalization of LNCs with CBD enhanced by 2.4-fold ($p < 0.01$) the *in vivo* brain targeting of their undecorated equally-sized counterparts. The increase in brain levels highly correlated with higher available plasma concentration and, in most cases, with lower recognition by the reticuloendothelial organs (Figure S2).

Remarkably, the enhancement in brain targeting achieved with the adsorption of CBD on LNCs outperformed by 6-fold that of the gluthatione functionalization strategy assessed in a seminal study with healthy mice that laid the foundations for the G-Technology® (the main brain active strategy that has already entered clinical trials for the treatment of brain diseases) (54). The brain targeting ability of CBD-decorated LNCs is likely mediated by receptor-mediated transcytosis across the brain endothelium (55). Among the many receptors located at the CNS level to which CBD binds, dopamine receptor has been reported to specifically locate at the BBB and has recently started being tested as a potential receptor to mediate brain targeting of nanocarriers with exogenous ligands (56).

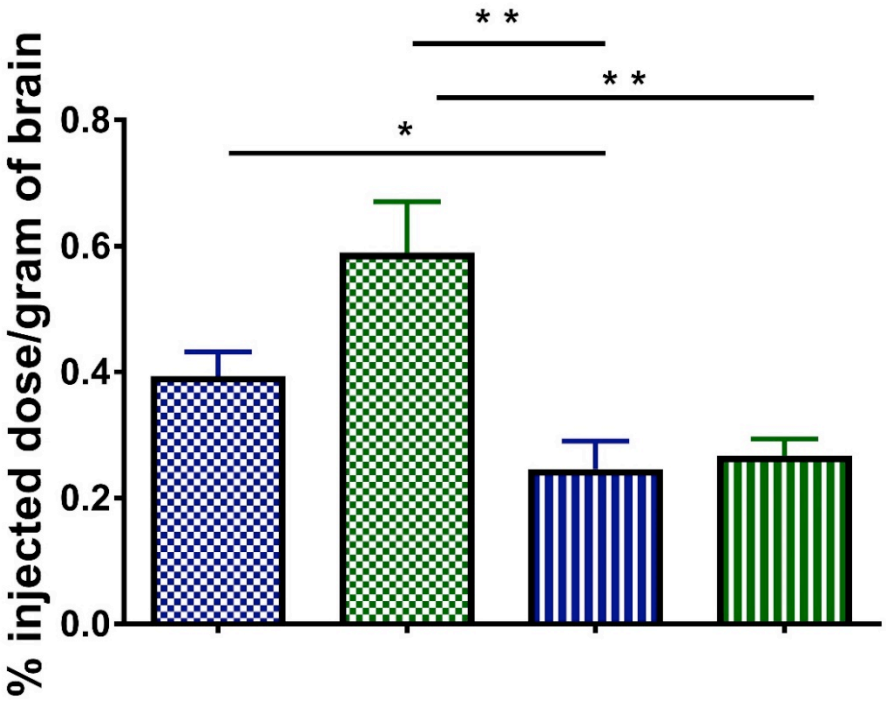

Figure 6: Quantitative analysis of the *in vivo* biodistribution of DiD-labeled LNCs in the brain of healthy mice expressed as percentage of the injected dose per gram of brain. The colours and fill patterns of the LNC formulations correspond to those of figure 2. *: p<0.05, **: p<0.01, ***: p<0.001.

Altogether, the consistency between the *in vitro* and *in vivo* results served to validate our *in vitro* BBB model with the human brain endothelial cell line hCMEC/D3 as a versatile screening method to evaluate the passage of nanocarriers across the BBB that meets the high-throughput demands in the early stages of the drug discovery and lacks ethical constraints.

Analogously, the glioma targeting ability has been evaluated through uptake experiments conducted with the human glioblastoma cell line U373MG. To this end, we have utilized the same LNCs than for the BBB-targeting ability (Figure 2).

The quantitative analysis of the *in vitro* glioma-targeting ability is also shown in Figure 3. A decrease in particle size consistently yielded a higher *in vitro* uptake by human glioblastoma cells (3.0-fold for undecorated LNCs, $p<0.05$ and 3.5-fold for CBD-adsorbed LNCs, $p<0.001$). Given the effect of particle size on the cell uptake, the influence of CBD adsorption was then assessed from a comparison of equally-sized LNCs. The functionalization of LNCs with CBD enhanced by 3.4-fold ($p < 0.001$) the *in vitro* glioma targeting properties of their equally-sized undecorated counterparts. The 3D reconstruction from the Z-stacks of the images taken by confocal microscopy further support qualitatively the internalization of LNCs within the U373MG cells (Figure 7).

The enhancement in glioma targeting achieved with the adsorption of CBD on LNCs equals that observed with other targeting moieties such as the aptamer AS1411 (57) or angiopep-2 (58) and outperformed that reported for transferrin (59), T7 peptide (60) or mannose (59). The exogenous and non-peptide nature of CBD makes it less prone to develop competitive phenomena with physiological ligands or cause immunogenicity.

A comparison of the uptake studies with both cell lines reveals that the enhancements in the targeting effects achieved with the reduction in LNC size ($p < 0.05$ for undecorated LNCs and $p< 0.001$ for CBD-functionalized LNCs) and CBD adsorption ($p < 0.001$) were statistically more significant with the human glioblastoma cells (Figure 3).

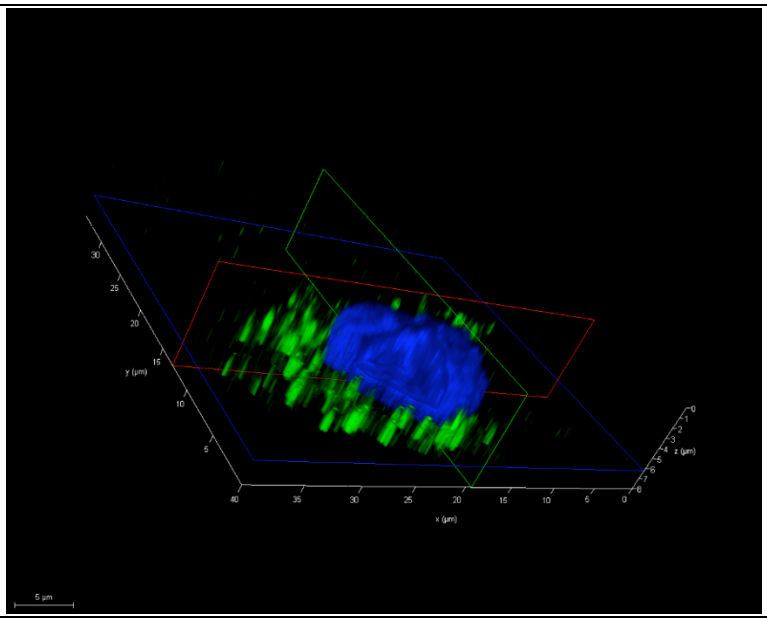

Figure 7: Example of 3D reconstruction from the Z-stacks of the images taken by confocal microscopy for DiO-labeled LNCs within U373MG cells.

3.3. Determination of the in vitro efficacy of CBD-loaded LNCs as extended-release carriers against U373MG cells

Monodisperse LNCs with the Labrafac®-Kolliphor® HS15 tandem loaded with CBD at a concentration of 15 % CBD/ Labrafac® WL1349 (w/w) were prepared in two different sizes for *in vitro* efficacy experiments under the assumption that LNCs contribute to overcome classical formulation problems associated with cannabinoids (61) and to attain a prolonged-release platform for this drug. The liquid lipid core of triglyceride oils was chosen on the grounds of the solubility of CBD to achieve both high encapsulation efficiencies and drug loading (Table S1).

Concerning particle size, the encapsulation of CBD followed the inverse pattern than its adsorption: the percentage increase in particle size in comparison to their blank counterparts was more evident for the bigger LNCs (Figure 8). These results positively correlated with the percentage of CBD loading, which ranged from 4.30% for the smaller LNCs to 7.66% for the bigger ones (Table S1). Moreover, in agreement with the hypothesized encapsulation, the zeta potential profiles were not changed in comparison to those obtained for blank LNCs (Figure S1): values close to neutrality with high profile width were obtained in all cases.

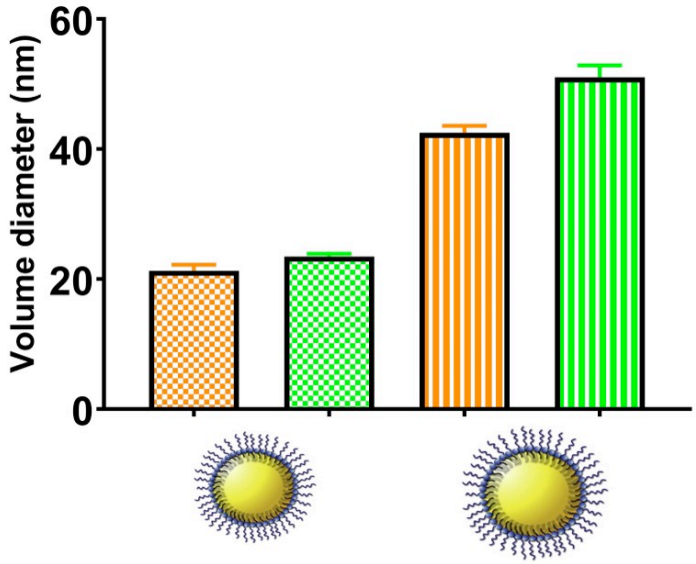

Figure 8: Average volume diameter of the different LNCs used to assess the *in vitro* efficacy against glioma: blank LNCs (orange) and CBD-loaded LNCs (pistachio). The smaller-sized formulation of each type has a squared fill pattern, whereas the bigger-sized has a striped fill pattern.

The results from cell viability experiments are shown in Figure 9. Noticeably, none of the formulations of blank LNCs utilized as controls showed significant cytotoxicity against the U373MG cell line within the evaluated concentration range according to ISO 10993-5 (Biological evaluation of medical devices, Part 5: Tests for *in vitro* cytotoxicity). Therefore, all changes in the percentage of cell viability following treatment with CBD-loaded LNCs can be attributed to the extent of CBD released from the LNCs at each time point.

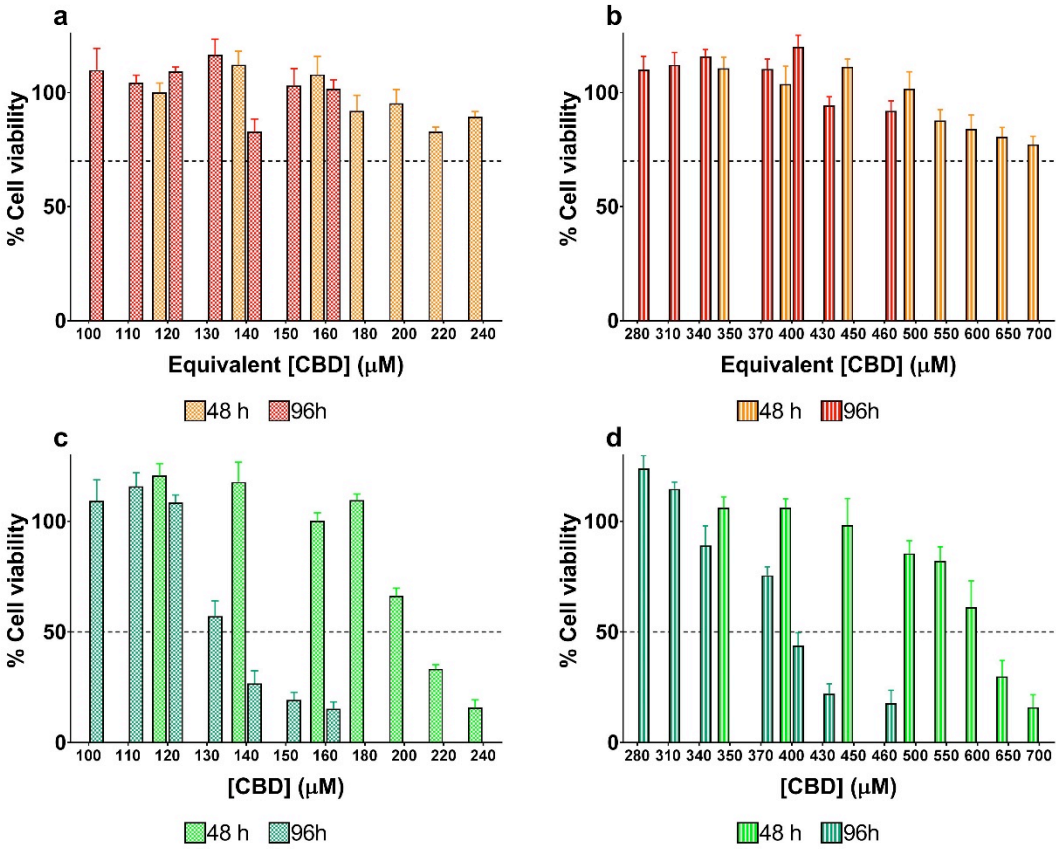

Figure 9: Cytotoxicity of blank LNCs and CBD-loaded LNCs in different sizes against the human glioblastoma U373MG cell line. (a) Cytotoxicity of 20 nm-sized blank LNCs after 48 (orange) and 96 hours (red). (b) Cytotoxicity of 40 nm-sized blank LNCs after 48 (orange) and 96 hours (red). (c) Cytotoxicity of 20 nm-sized CBD-loaded LNCs after 48 (pistachio) and 96 hours (dark green). (d) Cytotoxicity of 40 nm-sized blank LNCs after 48 (pistachio) and 96 hours (dark green).

Free CBD showed a clear antiproliferative effect against the glioblastoma cells (IC_{50} = 29.1 μM, Figure S3). The encapsulation of CBD considerably increased this IC_{50} value, as free CBD is readily available, whereas encapsulated CBD must be first released from the oily core of LNCs to exert its cytotoxic effect on glioma cells. Similar trends have been described for other drug-loaded carriers (56, 62, 63).

The size of LNCs played a key role in the extent of CBD release and subsequent cytotoxicity: the smaller-sized CBD-loaded LNCs reduced by 3.0-fold the IC_{50} value achieved with the bigger-sized CBD-loaded LNCs both after 48 (202.6 μM versus 615.4 μM) and 96 hours (129.1 μM versus 375.4 μM). Moreover, as deduced from the reduction in the IC_{50} values from 48 to 96 hours, LNCs continued to release CBD. Accordingly, CBD-loaded LNCs act as efficient extended-release carriers with great potential for glioma therapy.

4. CONCLUSIONS

The results presented herein serve to envision LNCs, prepared by the PIT method and loaded with CBD in their oily core and functionalized with CBD on their surface, as promising dually-targeted candidates for intravenous treatment of glioma. We have introduced, on the one hand, a pioneering functionalization strategy for brain tumor targeting of LNCs with this non-immunogenic and non-psychotropic cannabinoid (with better targeting properties than some other targeting strategies that have already reached the clinical trials stage) and, on the other hand, nanocapsules as extended-release carriers of CBD at high drug loading to overcome the formulation issues usually associated with cannabinoids that have heretofore constrained their therapeutic potential. Moreover, to contribute to the rational design of nanocapsules, we have demonstrated that both the BBB and glioma targeting ability and the drug release rate can be tailored by varying

the particle size of LNCs. This fine size-tailoring can be achieved by the PIT method thanks to the herein-described linear univariate mathematical model as a function of the oily phase/surfactant mass ratio to increase the chances of success in the development of nanomedicines for the treatment of glioma and other brain diseases. Consequently, they deserve subsequent *in vivo* evaluation in an animal model of disease.

Acknowledgements

This work was supported by the Complutense Research Fund (Ref. 16/83) and by the Santander-UCM Research Group GR35/10: Parenteral Administration of Drugs. J. A.-B. would like to thank the Spanish Ministry of Education for his contract within the Professor Training Program FPU (Ref. FPU13/02325) and for funding two research stays at the School of Life, Health and Chemical Sciences, The Open University (Refs. EST15/00534 and EST16/00556) and a research stay at L'unité Micro et Nanomédecines Biomimétiques (MINT) INSERM 1066 CNRS 6021, Université d'Angers (Ref. EST14/00229).

Conflict of interest

The authors declare no competing interests

5. REFERENCES

1. Silberberg D, Anand NP, Michels K, Kalaria RN. Brain and other nervous system disorders across the lifespan - global challenges and opportunities. Nature. 2015;527:S151-S4.
2. Oberoi RK, Parrish KE, Sio TT, Mittapalli RK, Elmquist WF, Sarkaria JN. Strategies to improve delivery of anticancer drugs across the blood-brain barrier to treat glioblastoma. Neuro-Oncology. 2016;18:27-36.
3. Tsou YH, Zhang XQ, Zhu H, Syed S, Xu XY. Drug Delivery to the Brain across the Blood-Brain Barrier Using Nanomaterials. Small. 2017;13:1701921.
4. Zhou YQ, Peng ZL, Seven ES, Leblanc RM. Crossing the blood-brain barrier with nanoparticles. Journal of Controlled Release. 2018;270:290-303.
5. Kaushik A, Jayant RD, Bhardwaj V, Nair M. Personalized nanomedicine for CNS diseases. Drug discovery today. 2018;23:1007-15.
6. Liebner S, Dijkhuizen RM, Reiss Y, Plate KH, Agalliu D, Constantin G. Functional morphology of the blood-brain barrier in health and disease. Acta Neuropathologica. 2018;135:311-36.
7. Roger K. Nanoemulsification in the vicinity of phase inversion: Disruption of bicontinuous structures in oil/surfactant/water systems. Current Opinion in Colloid & Interface Science. 2016;25:120-8.
8. Louis DN, Perry A, Reifenberger G, von Deimling A, Figarella-Branger D, Cavenee WK, et al. The 2016 World Health Organization Classification of Tumors of the Central Nervous System: a summary. Acta Neuropathologica. 2016;131:803-20.
9. Alifieris C, Trafalis DT. Glioblastoma multiforme: Pathogenesis and treatment. Pharmacology & Therapeutics. 2015;152:63-82.
10. Velasco G, Hernandez-Tiedra S, Davila D, Lorente M. The use of cannabinoids as anticancer agents. Progress in Neuro-Psychopharmacology & Biological Psychiatry. 2016;64:259-66.
11. Fowler CJ. Delta(9)-Tetrahydrocannabinol and Cannabidiol as Potential Curative Agents for Cancer: A Critical Examination of the Preclinical Literature. Clinical Pharmacology & Therapeutics. 2015;97:587-96.
12. Andre CM, Hausman JF, Guerriero G. Cannabis sativa: The Plant of the Thousand and One Molecules. Frontiers in Plant Science. 2016;7:19.
13. Russo EB. Beyond Cannabis: Plants and the Endocannabinoid System. Trends in Pharmacological Sciences. 2016;37:594-605.
14. Pisanti S, Malfitano AM, Ciaglia E, Lamberti A, Ranieri R, Cuomo G, et al. Cannabidiol: State of the art and new challenges for therapeutic applications. Pharmacol Ther. 2017;175:133-50.
15. Xie JR, Xiao DJ, Zhao JN, Hu NQ, Bao Q, Jiang L, et al. Mesoporous Silica Particles as a Multifunctional Delivery System for Pain Relief in Experimental Neuropathy. Advanced Healthcare Materials. 2016;5:1213-21.
16. Martin-Banderas L, Munoz-Rubio I, Prados J, Alvarez-Fuentes J, Calderon-Montano JM, Lopez-Lazaro M, et al. In vitro and in vivo evaluation of Delta(9)-tetrahidrocannabinol/PLGA nanoparticles for cancer chemotherapy. International Journal of Pharmaceutics. 2015;487:205-12.
17. Martin-Banderas L, Munoz-Rubio I, Alvarez-Fuentes J, Duran-Lobato M, Arias JL, Holgado MA, et al. Engineering of Delta(9)-tetrahydrocannabinol delivery systems based on surface modified-PLGA nanoplatforms. Colloids and Surfaces B-Biointerfaces. 2014;123:114-22.
18. Cherniakov I, Izgelov D, Barasch D, Davidson E, Domb AJ, Hoffman A. Piperine-pro-nanolipospheres as a novel oral delivery system of cannabinoids: Pharmacokinetic evaluation in healthy volunteers in comparison to buccal spray administration. Journal of Controlled Release. 2017;266:1-7.
19. Ligresti A, De Petrocellis L, de la Ossa DHP, Aberturas R, Cristino L, Moriello AS, et al. Exploiting Nanotechnologies and TRPV1 Channels to Investigate the Putative Anandamide Membrane Transporter. Plos One. 2010;5:12.
20. Esposito E, Ravani L, Drechsler M, Mariani P, Contado C, Ruokolainen J, et al. Cannabinoid antagonist in nanostructured lipid carriers (NLCs): design, characterization and in vivo study. Materials Science & Engineering C-Materials for Biological Applications. 2015;48:328-36.

21. Esposito E, Drechsler M, Cortesi R, Nastruzzi C. Encapsulation of cannabinoid drugs in nanostructured lipid carriers. European Journal of Pharmaceutics and Biopharmaceutics. 2016;102:87-91.
22. Linsell O, Brownjohn PW, Nehoff H, Greish K, Ashton JC. Effect of styrene maleic acid WIN55,212-2 micelles on neuropathic pain in a rat model. Journal of Drug Targeting. 2015;23:353-9.
23. He XL, Yang L, Wang M, Zhuang XZ, Huang RQ, Zhu RR, et al. Targeting the Endocannabinoid/CB1 Receptor System For Treating Major Depression Through Antidepressant Activities of Curcumin and Dexanabinol-Loaded Solid Lipid Nanoparticles. Cellular Physiology and Biochemistry. 2017;42:2281-94.
24. Berrocoso E, Rey-Brea R, Fernandez-Arevalo M, Mico JA, Martin-Banderas L. Single oral dose of cannabinoid derivate loaded PLGA nanocarriers relieves neuropathic pain for eleven days. Nanomedicine-Nanotechnology Biology and Medicine. 2017;13:2623-32.
25. Duran-Lobato M, Martin-Banderas L, Goncalves LMD, Fernandez-Arevalo M, Almeida AJ. Comparative study of chitosan- and PEG-coated lipid and PLGA nanoparticles as oral delivery systems for cannabinoids. Journal of Nanoparticle Research. 2015;17:17.
26. Martin-Banderas L, Alvarez-Fuentes J, Duran-Lobato M, Prados J, Melguizo C, Fernandez-Arevalo M, et al. Cannabinoid derivate-loaded PLGA nanocarriers for oral administration: formulation, characterization, and cytotoxicity studies. International Journal of Nanomedicine. 2012;7:5793-806.
27. Duran-Lobato M, Martin-Banderas L, Lopes R, Goncalves LMD, Fernandez-Arevalo M, Almeida AJ. Lipid nanoparticles as an emerging platform for cannabinoid delivery: physicochemical optimization and biocompatibility. Drug Development and Industrial Pharmacy. 2016;42:190-8.
28. Sweeney MD, Sagare AP, Zlokovic BV. Blood-brain barrier breakdown in Alzheimer disease and other neurodegenerative disorders. Nature Reviews Neurology. 2018;14:133-50.
29. Sarkaria JN, Hu LS, Parney IF, Pafundi DH, Brinkmann DH, Laack NN, et al. Is the blood-brain barrier really disrupted in all glioblastomas? A critical assessment of existing clinical data. Neuro-Oncology. 2018;20:184-91.
30. Bertrand N, Wu J, Xu XY, Kamaly N, Farokhzad OC. Cancer nanotechnology: The impact of passive and active targeting in the era of modern cancer biology. Advanced Drug Delivery Reviews. 2014;66:2-25.
31. Oller-Salvia B, Sanchez-Navarro M, Giralt E, Teixido M. Blood-brain barrier shuttle peptides: an emerging paradigm for brain delivery. Chemical Society Reviews. 2016;45:4690-707.
32. Peluffo H, Unzueta U, Negro-Demontel ML, Xu ZK, Vaquez E, Ferrer-Miralles N, et al. BBB-targeting, protein-based nanomedicines for drug and nucleic acid delivery to the CNS. Biotechnology Advances. 2015;33:277-87.
33. Laprairie RB, Bagher AM, Kelly MEM, Denovan-Wright EM. Cannabidiol is a negative allosteric modulator of the cannabinoid CB1 receptor. British Journal of Pharmacology. 2015;172:4790-805.
34. Martinez-Pinilla E, Varani K, Reyes-Resina I, Angelats E, Vincenzi F, Ferreiro-Vera C, et al. Binding and Signaling Studies Disclose a Potential Allosteric Site for Cannabidiol in Cannabinoid CB2 Receptors. Frontiers in Pharmacology. 2017;8:10.
35. Espejo-Porras F, Fernandez-Ruiz J, Pertwee RG, Mechoulam R, Garcia C. Motor effects of the non-psychotropic phytocannabinoid cannabidiol that are mediated by 5-HT1A receptors. Neuropharmacology. 2013;75:155-63.
36. Nabissi M, Morelli MB, Amantini C, Liberati S, Santoni M, Ricci-Vitiani L, et al. Cannabidiol stimulates Aml-1a-dependent glial differentiation and inhibits glioma stem-like cells proliferation by inducing autophagy in a TRPV2-dependent manner. International Journal of Cancer. 2015;137:1855-69.
37. Xiong W, Cui TX, Cheng KJ, Yang F, Chen SR, Willenbring D, et al. Cannabinoids suppress inflammatory and neuropathic pain by targeting alpha 3 glycine receptors. Journal of Experimental Medicine. 2012;209:1121-34.
38. Mecha M, Feliu A, Inigo PM, Mestre L, Carrillo-Salinas FJ, Guaza C. Cannabidiol provides long-lasting protection against the deleterious effects of inflammation in a viral model of multiple sclerosis: A role for A(2A) receptors. Neurobiology of Disease. 2013;59:141-50.
39. Sylantyev S, Jensen TP, Ross RA, Rusakov DA. Cannabinoid- and lysophosphatidylinositol-sensitive receptor GPR55 boosts neurotransmitter release at central synapses. Proceedings of the National Academy of Sciences of the United States of America. 2013;110:5193-8.
40. Seeman P. Cannabidiol is a partial agonist at dopamine D2High receptors, predicting its antipsychotic clinical dose. Translational Psychiatry. 2016;6:e920.
41. Wu XY, Han LJ, Zhang XL, Li L, Jiang CZ, Qiu Y, et al. Alteration of endocannabinoid system in human gliomas. Journal of Neurochemistry. 2012;120:842-9.
42. Andradas C, Caffarel MM, Perez-Gomez E, Salazar M, Lorente M, Velasco G, et al. The orphan G protein-coupled receptor GPR55 promotes cancer cell proliferation via ERK. Oncogene. 2011;30:245-52.
43. Huynh NT, Passirani C, Saulnier P, Benoit JP. Lipid nanocapsules: A new platform for nanomedicine. International Journal of Pharmaceutics. 2009;379:201-9.

44. Aparicio-Blanco J, Martin-Sabroso C, Torres-Suarez AI. In vitro screening of nanomedicines through the blood brain barrier: A critical review. Biomaterials. 2016;103:229-55.
45. Morales D, Gutierrez JM, Garcia-Celma MJ, Solans YC. A study of the relation between bicontinuous microemulsions and oil/water nano-emulsion formation. Langmuir. 2003;19:7196-200.
46. Izquierdo P, Esquena J, Tadros TF, Dederen JC, Feng J, Garcia-Celma MJ, et al. Phase behavior and nano-emulsion formation by the phase inversion temperature method. Langmuir. 2004;20:6594-8.
47. Anton N, Vandamme TF. The universality of low-energy nano-emulsification. International Journal of Pharmaceutics. 2009;377:142-7.
48. Chuesiang P, Siripatrawan U, Sanguandeekul R, McLandsborough L, McClements DJ. Optimization of cinnamon oil nanoemulsions using phase inversion temperature method: Impact of oil phase composition and surfactant concentration. Journal of Colloid and Interface Science. 2018;514:208-16.
49. Sadurni N, Solans C, Azemar N, Garcia-Celma MJ. Studies on the formation of O/W nano-emulsions, by low-energy emulsification methods, suitable for pharmaceutical applications. European Journal of Pharmaceutical Sciences. 2005;26:438-45.
50. Caldero G, Garcia-Celma MJ, Solans C. Formation of polymeric nano-emulsions by a low-energy method and their use for nanoparticle preparation. Journal of Colloid and Interface Science. 2011;353:406-11.
51. Morral-Ruiz G, Melgar-Lesmes P, Garcia ML, Solans C, Garcia-Celma MJ. Polyurethane and polyurea nanoparticles based on polyoxyethylene castor oil derivative surfactant suitable for endovascular applications. International Journal of Pharmaceutics. 2014;461:1-13.
52. Elgammal M, Schneider R, Gradzielski M. Preparation of latex nanoparticles using nanoemulsions obtained by the phase inversion composition (PIC) method and their application in textile printing. Colloids and Surfaces a-Physicochemical and Engineering Aspects. 2015;470:70-9.
53. Balzeau J, Pinier M, Berges R, Saulnier P, Benoit JP, Eyer J. The effect of functionalizing lipid nanocapsules with NFL-TBS.40-63 peptide on their uptake by glioblastoma cells. Biomaterials. 2013;34:3381-9.
54. Gaillard PJ, Appeldoorn CCM, Dorland R, van Kregten J, Manca F, Vugts DJ, et al. Pharmacokinetics, Brain Delivery, and Efficacy in Brain Tumor-Bearing Mice of Glutathione Pegylated Liposomal Doxorubicin (2B3-101). Plos One. 2014;9:e82331.
55. Bih CI, Chen T, Nunn AVW, Bazelot M, Dallas M, Whalley BJ. Molecular Targets of Cannabidiol in Neurological Disorders. Neurotherapeutics. 2015;12:699-730.
56. Belhadj Z, Ying M, Cao X, Hu XF, Zhan CY, Wei XL, et al. Design of Y-shaped targeting material for liposome-based multifunctional glioblastoma-targeted drug delivery. Journal of Controlled Release. 2017;255:132-41.
57. Luo ZM, Yan ZQ, Jin K, Pang Q, Jiang T, Lu H, et al. Precise glioblastoma targeting by AS1411 aptamer-functionalized poly (L-gamma-glutamylglutamine)-paclitaxel nanoconjugates. Journal of Colloid and Interface Science. 2017;490:783-96.
58. Luo ZM, Jin K, Pang Q, Shen S, Yan ZQ, Jiang T, et al. On-Demand Drug Release from Dual-Targeting Small Nanoparticles Triggered by High-Intensity Focused Ultrasound Enhanced Glioblastoma-Targeting Therapy. Acs Applied Materials & Interfaces. 2017;9:31612-25.
59. Ying X, Wen H, Lu WL, Du J, Guo J, Tian W, et al. Dual-targeting daunorubicin liposomes improve the therapeutic efficacy of brain glioma in animals. Journal of Controlled Release. 2010;141:183-92.
60. Wei L, Guo XY, Yang T, Yu MZ, Chen DW, Wang JC. Brain tumor-targeted therapy by systemic delivery of siRNA with Transferrin receptor-mediated core-shell nanoparticles. International Journal of Pharmaceutics. 2016;510:394-405.
61. Holgado MA, Martin-Banderas L, Alvarez-Fuentes J, Fernandez-Arevalo M. Neuroprotective effect of cannabinoids nanoplatforms in neurodegenerative diseases. Journal of Drug Delivery Science and Technology. 2017;42:84-93.
62. Chen CT, Duan ZQ, Yuan Y, Li RX, Pang L, Liang JM, et al. Peptide-22 and Cyclic RGD Functionalized Liposomes for Glioma Targeting Drug Delivery Overcoming BBB and BBTB. Acs Applied Materials & Interfaces. 2017;9:5864-73.
63. Wei XL, Gao J, Zhan CY, Xie C, Chai ZL, Ran D, et al. Liposome-based glioma targeted drug delivery enabled by stable peptide ligands. Journal of Controlled Release. 2015;218:13-21.

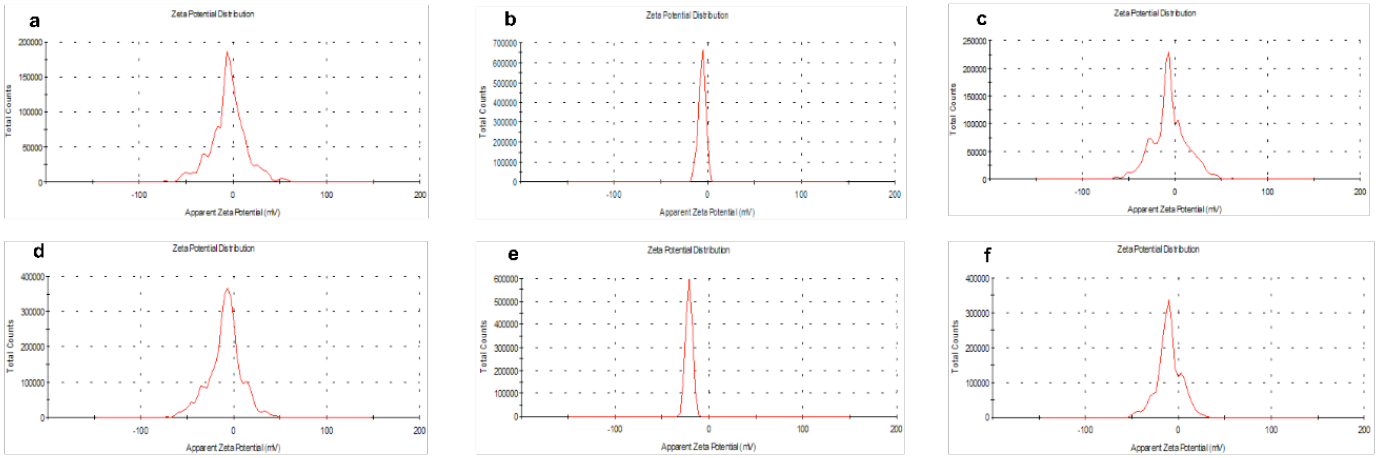

Supporting information

Figure S1: Zeta potential profiles for blank LNCs (a: smaller-sized formulation and d: bigger-sized formulation), CBD-decorated LNCs (b: smaller-sized formulation and e: bigger-sized formulation) and CBD-encapsulated LNCs (c: smaller-sized formulation and f: bigger-sized formulation).

Table S1: CBD adsorption/encapsulation efficiencies (AE/EE) and drug content (DC) of the different LNCs discussed in the manuscript.

LNC formulation	AE/EE (%)	DC (%)
Smaller-sized CBD-adsorbed LNCs	96.99 ± 2.58	1.55 ± 0.07
Bigger-sized CBD-adsorbed LNCs	95.97 ± 4.72	2.17 ± 0.06
Smaller-sized CBD-encapsulated LNCs	96.75 ± 1.45	4.30 ± 0.07
Bigger-sized CBD-encapsulated LNCs	96.43 ± 3.25	7.66 ± 0.30

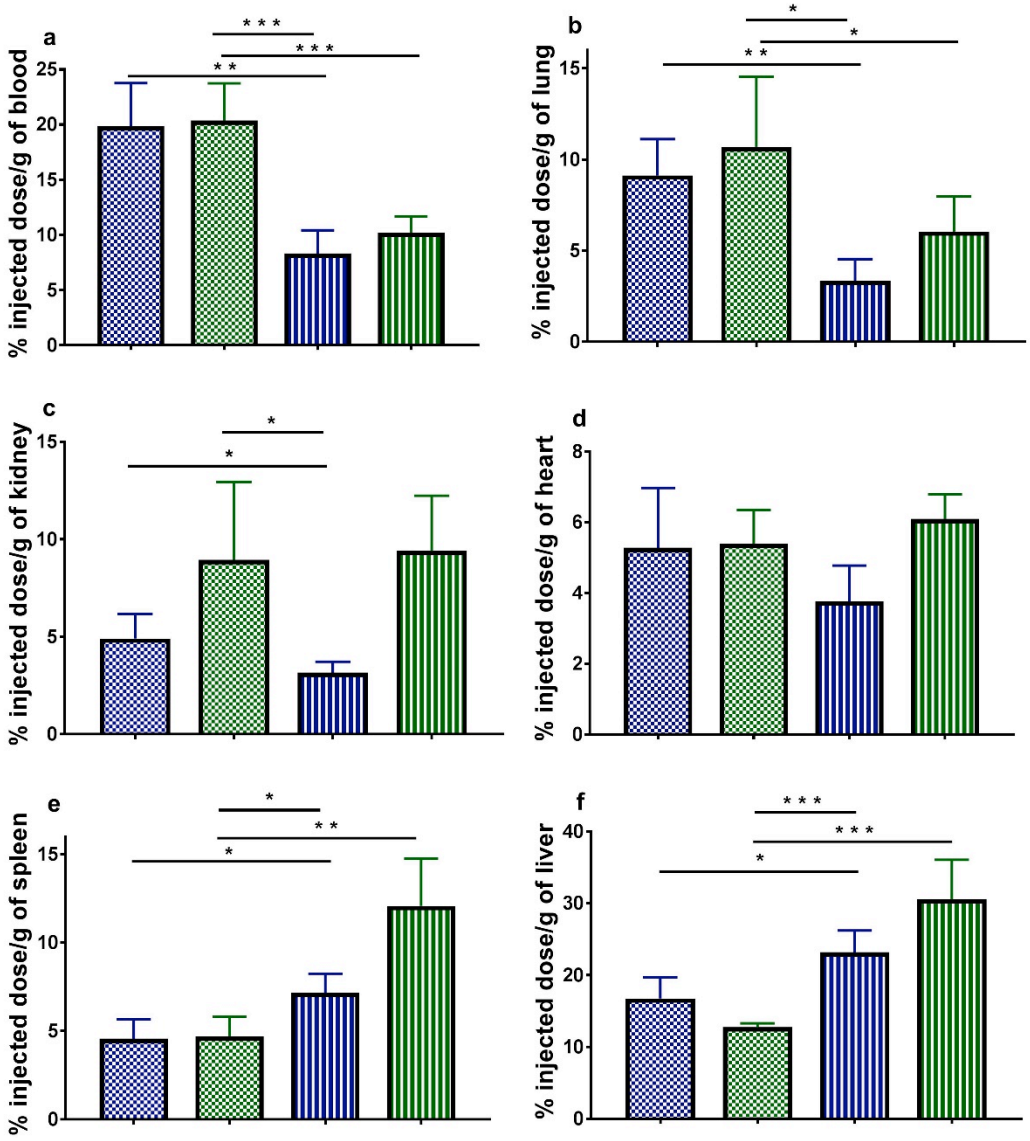

Figure S2: Quantitative analysis of the *in vivo* biodistribution of DiD-labeled LNCs in healthy mice expressed as percentage of the injected dose per gram of organ: (a) blood, (b) lungs, (c) kidneys, (d) heart, (e) spleen and (f) liver. The colours and fill patterns of the LNC formulations correspond to those of figure 2. *: p<0.05, **: p<0.01, ***: p<0.001.

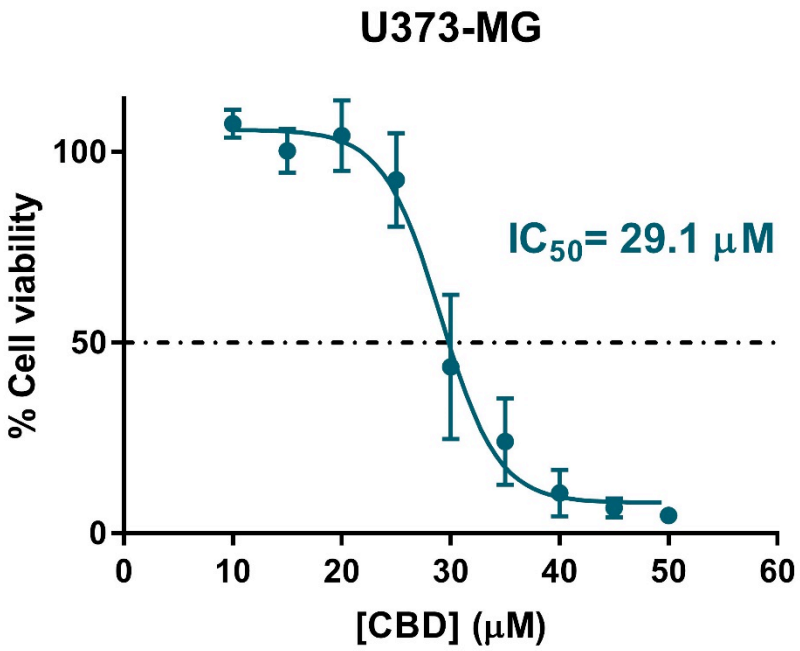

Figure S3: Antiproliferative effect of free CBD against the human glioblastoma U373MG cell line.